Received: 3 January 2021 | Revised: 9 April 2021 | Accepted: 12 April 2021

DOI: 10.1111/jnc.15367

ORIGINAL ARTICLE

Journal of Neurochemistry JNC The Official Journal of the International Society for Neurochemistry WILEY

# Inhibition of CD38 and supplementation of nicotinamide riboside ameliorate lipopolysaccharide-induced microglial and astrocytic neuroinflammation by increasing $NAD^+$

Jureepon Roboon[1] | Tsuyoshi Hattori[1] | Hiroshi Ishii[1] | Mika Takarada-Iemata[1] | Dinh Thi Nguyen[1] | Collin D. Heer[2] | Denis O'Meally[3] | Charles Brenner[4] | Yasuhiko Yamamoto[5] | Hiroshi Okamoto[5,6] | Haruhiro Higashida[7] | Osamu Hori[1]

[1]Department of Neuroanatomy, Graduate School of Medical Sciences, Kanazawa University, Kanazawa, Japan

[2]Free Radical and Radiation Biology Program, University of Iowa, Iowa City, IA, USA

[3]Center for Gene Therapy, Beckman Research Institute, City of Hope National Medical Center, Duarte, CA, USA

[4]Department of Diabetes & Cancer Metabolism, Beckman Research Institute, City of Hope National Medical Center, Duarte, CA, USA

[5]Department of Biochemistry and Molecular Vascular Biology, Graduate School of Medical Sciences, Kanazawa University, Kanazawa, Japan

[6]Department of Biochemistry, Tohoku University Graduate School of Medicine, Sendai, Japan

[7]Research Center for Child Mental Development, Kanazawa University, Kanazawa, Japan

**Correspondence**
Tsuyoshi Hattori, Department of Neuroanatomy, Kanazawa University Graduate School of Medical Sciences, 13-1 Takara-Machi, Kanazawa City, Ishikawa, 920-8640, Japan
Email: thattori@staff.kanazawa-u.ac.jp

**Funding information**
Grant-in Aid for Scientific Research, Grant/Award Number: 18KK0435, 18K06501, 18KK0255, 18K06500 and 18K06463; Ministry of Education, Science, Technology, Sports and Culture of Japan; Alfred E. Mann Family Foundation; National Cancer Institute, Grant/Award Number: F99CA245722; Kanazawa University

## Abstract

Neuroinflammation is initiated by activation of the brain's innate immune system in response to an inflammatory challenge. Insufficient control of neuroinflammation leads to enhanced or prolonged pathology in various neurological conditions including multiple sclerosis and Alzheimer's disease. Nicotinamide adenine dinucleotide ($NAD^+$) plays critical roles in cellular energy metabolism and calcium homeostasis. Our previous study demonstrated that deletion of CD38, which consumes $NAD^+$, suppressed cuprizone-induced demyelination, neuroinflammation, and glial activation. However, it is still unknown whether CD38 directly affects neuroinflammation through regulating brain $NAD^+$ level. In this study, we investigated the effect of CD38 deletion and inhibition and supplementation of $NAD^+$ on lipopolysaccharide (LPS)-induced neuroinflammation in mice. Intracerebroventricular injection of LPS significantly increased CD38 expression especially in the hippocampus. Deletion of CD38 decreased LPS-induced inflammatory responses and glial activation. Pre-administration of apigenin, a flavonoid with CD38 inhibitory activity, or nicotinamide riboside (NR), an $NAD^+$ precursor, increased $NAD^+$ level, and significantly suppressed induction of cytokines and chemokines, glial activation and subsequent neurodegeneration after LPS administration. In cell culture, LPS-induced inflammatory responses were suppressed by treatment of primary astrocytes or microglia with apigenin, $NAD^+$, NR or 78c, the latter

**Abbreviations:** BBB, Blood–brain barrier; cADPR, cyclic ADP-ribose; CCL2, C-C motif chemokine ligand 2; CCL3, C-C motif chemokine ligand 3; CNS, central nervous system; CX, cortex; DAPI, 4',6-diamidino-2-phenylindole dihydrochloride; GAPDH, glyceraldehyde 3-phosphate dehydrogenase; GFAP, glial fibrillary acidic protein; HPC, hippocampus; i.c.v., intracerebroventricular; i.p., intraperitoneal; Iba1, ionized calcium-binding adaptor molecule 1; Il1b, interleukin 1 beta; Il6, interleukin 6; LPS, lipopolysaccharide; MAP2, microtubule-associated protein 2; NA, nicotinic acid; $NAD^+$, nicotinamide adenine dinucleotide; NAM, nicotinamide; NF-κB, nuclear factor-kappa B; Nos2, nitric oxide synthase 2; NR, nicotinamide riboside; PARPs, poly (ADP-ribose) polymerases; PBS, phosphate-buffered saline; PFA, paraformaldehyde; RRID, Research Resource Identifier (see scicrunch.org); RT-qPCR, reverse transcription quantitative polymerase chain reaction; TNF, tumor necrosis factor.

  

a specific CD38 inhibitor. Finally, all these compounds suppressed NF-κB signaling pathway in microglia. These results suggest that CD38-mediated neuroinflammation is linked to $NAD^+$ consumption and that boosting $NAD^+$ by CD38 inhibition and NR supplementation directly suppress neuroinflammation in the brain.

**KEYWORDS**

apigenin, astrocyte, LPS, microglia, neurodegeneration, neuroinflammation, NR

## 1 | INTRODUCTION

Neuroinflammation is a biological response initiated by tissue injury or infection in the central nervous system (CNS) to eliminate pathogenic components and induce tissue remodeling. However, insufficient control of neuroinflammation leads to the progression of many neurological conditions such as multiple sclerosis, traumatic brain injury, and Alzheimer's disease (Akiyama et al., 2000; Frischer et al., 2009; Lucas et al., 2006). Glial cells, including microglia and astrocytes, are involved in the immune response in the CNS and play important roles in the development of neuroinflammation. It is well documented that sustained inflammatory responses cause the release of harmful mediators such as cytokines and chemokines from activated glial cells, and further affect neuronal cells by triggering neurodegeneration (Jo et al., 2017; Lian et al., 2016; Liu et al., 2011; Norden et al., 2016). Therefore, suppression of neuroinflammation may be an important therapeutic target in neurological diseases.

CD38 is a type II and type III transmembrane protein (Zhao et al., 2012) that catalyzes the formation of cyclic ADP-ribose (cADPR) and nicotinic acid adenine dinucleotide phosphate ($NAADP^+$) from nicotinamide adenine dinucleotide ($NAD^+$) and related metabolites (Hogan et al., 2019) to mobilize calcium from intracellular stores (Guse, 2005; Hogan et al., 2019; Lee, 2004; Malavasi et al., 2008; Nam et al., 2020; Takasawa et al., 1993b, Takasawa, Tohgo et al., 1993). CD38 has diverse functions. For example, it promotes the secretion of insulin from pancreatic beta cells and oxytocin from hypothalamic neurons, thereby promoting social behaviors that are deficient in mouse models of autism spectrum disorder (ASD) (Gerasimenko et al., 2020; Higashida et al., 2012; Jin et al., 2007; Kim et al., 2016; Okamoto et al., 2017; Takasawa et al., 1993a). CD38 is also associated with glial cell functions. We previously demonstrated that under physiological conditions, CD38 regulates the maturation of astrocytes and differentiation of oligodendrocyte precursor cells using $NAD^+$ in the brain (Hattori et al., 2017). We also recently discovered that CD38 is crucially involved in the cuprizone-induced demyelination model in mice. CD38 expression was increased in the brain after cuprizone administration in a manner associated with the production of pro-inflammatory molecules, glial activation, and subsequent neurodegeneration. Deletion of CD38 suppresses these phenotypes by increasing $NAD^+$ levels in the brain (Roboon et al., 2019). CD38 has also been reported to play a critical role in the pathology of experimental autoimmune encephalomyelitis, another model of demyelination in mice (Herrmann et al., 2016).

$NAD^+$ is synthesized in four gene-encoded biosynthetic pathways from tryptophan, nicotinic acid (NA), nicotinamide (NAM), and nicotinamide riboside (NR) (Bieganowski & Brenner, 2004; Bogan & Brenner, 2008). The NR biosynthetic pathway is both unique and highly efficient in rodents and humans (Trammell et al., 2016) and corresponds to a biosynthetic pathway that is transcriptionally induced in heart failure (Diguet et al., 2018) and central brain injury (Vaur et al., 2017). Moreover in an Alzheimer's disease model, NR improved both cognitive function and protected against neurodegeneration (Gong et al., 2013; Hou et al., 2018). These studies suggest that $NAD^+$ has suppressive effect on neuroinflammation, but it has not been tested directly using neuroinflammation mouse model.

The $NAD^+$ level in the brain can also be increased by compounds that depress $NAD^+$ consumption. Thiazoloquin(az)olin(on)e, 78c, is a chemical that has a specific inhibitory effect on CD38 activity (CD38i) and has been reported to arrest age-related $NAD^+$ decline (Chini et al., 2020; Tarrago et al., 2018). Similarly, a natural flavonoid apigenin (4'5,7-trihydroxyflavone) (Nijveldt et al., 2001; Shukla & Gupta, 2010; Venigalla et al., 2015), was reported to inhibit CD38 enzymatic activity and increase intracellular $NAD^+$ levels (Escande et al., 2013). In this study, to clarify roles of CD38 and $NAD^+$ for neuroinflammation in the brain, we investigated the anti-inflammatory effects of $NAD^+$ on lipopolysaccharide (LPS)-induced neuroinflammation by inhibition of CD38 and supplementation of NR.

## 2 | MATERIALS AND METHODS

### 2.1 | Chemicals

The chemicals used in this study were as follows: LPS (Cat. No. 20389-04, Nacalai Tesque), β-$NAD^+$ (Cat. No. 24334-97, Nacalai Tesque), nicotinamide riboside (Cat. No. ASB-00014315, ChromaDex), apigenin (Cat. No. 016-18913, Wako), and compound 78c (Cat. No. 538763; Calbiochem).

### 2.2 | Animals and treatments

Wild-type (WT) and CD38 knockout (KO) male ICR mice (10–11 week old) were used for the experiments (body weight; 30–36 g) ($n = 260$).

CD38 KO mice were generated as described previously and backcrossed for more than eight times (Kato et al., 1999). This study was not pre-registered and no randomization/blinding was performed. No exclusion criteria were pre-determined, and no animals were excluded. Sample size for each experiment was determined based on our previous studies (Roboon et al., 2019). All mice were housed in 345 × 168 × 140 mm cages in a temperature-controlled room (24–25°C) with 12-hr light-dark cycles. Food and water were available ad libitum. All the animal experiments were performed between10:00 a.m. and 5:00 p.m. LPS injection was performed as described previously (Zhao et al., 2019). Mice were anesthetized with a mixture of anesthetic, muscle relaxant, analgesic, and sedative such as medetomidine (0.3 mg/kg; Domitor®; Nippon Zenyaku Kogyo), butorphanol (5.0 mg/kg; Vetorphale®; Meiji Seika Pharma), and midazolam (4.0 mg/kg; Midazolam Sandoz®; Sandoz) to minimize the pain. 10 μg LPS dissolved in 5 μL of sterile PBS or control sterile PBS was injected into the right lateral cerebral ventricle (0.3 mm caudal to bregma and −1.0 mm from lateral to midline at a depth of 3.0 mm) using a microsyringe and stereotaxic coordinates. Apigenin (40 mg/kg) or NR (400 mg/kg) was administered intraperitoneally once per day for seven consecutive days, followed by LPS injection 6 hr after the final administration of apigenin or NR. The mice were deeply anesthetized with isoflurane (1ml/ml, Cat. No. 26675-46-7, Fujifilm Wako Pure Chemical Industries. Ltd.) and sacrificed at the indicated times after LPS injection. To avoid the effect of injection-mediated brain damage, the contralateral (left) side of the cerebral cortex or hippocampus was analyzed in all experiments. All animal experiments were performed in accordance with the guidelines and approved by the Animal Care and Use Committee of Kanazawa University (AP-194042).

## 2.3 | Reverse transcription quantitative polymerase chain reaction (RT-QPCR)

RT-qPCR was performed as described previously (Hattori et al., 2010). In brief, total RNA was extracted from the cerebral cortex, hippocampus, or cultured cells using the FASTGene™ RNA Basic Kit. (Cat. No. FG-80250; Nippon Genetics Co., Ltd), and cDNA was synthesized using the High-Capacity cDNA Reverse Transcription Kit (Cat. No. 4368814; Applied Biosystems). Individual cDNA sequences were amplified using the Thunderbird™ SYBR qPCR® Mix (Cat. No. QPS-201; Toyobo Co. Ltd.) with specific primers. To measure differential expression, the comparative Ct method was used for data analyses in MxPro 4.10 (Agilent Technologies Inc.). The primer sequences are listed in Table S1.

## 2.4 | Western blot analyses

The hippocampal tissues or cultured cells were homogenized in a RIPA lysis buffer containing 1% NP-40, 0.1% sodium dodecyl sulfate (SDS), 0.2% deoxycholate, and protease inhibitors (1 mM phenylmethylsulfonyl fluoride, 1 μg/ml aprotinin), and then centrifuged at 17,000 *g* for 15 min. Denatured protein lysates were electrophoretically separated using SDS-polyacrylamide gel electrophoresis and proteins were transferred onto polyvinylidene fluoride membranes. Membranes were blocked in 5% skimmed milk for 30 min and incubated with anti-CD38 (RRID:AB_1241945; R and D systems, 1:500), anti-glial fibrillary acidic protein (GFAP) (RRID:AB_477035; Sigma-Aldrich, 1:2000), anti-ionized calcium binding adaptor molecule 1 (Iba1) (RRID:AB_839504; Fujifilm Wako Pure Chemical Industries. Ltd, 1:1,000), p-Stat3 (Tyr705) (RRID:AB_2491009; Cell Signaling Technology) and Stat3 (RRID:AB_331588; Cell Signaling Technology) antibodies for 16 hr at 4°C. Membranes were washed several times with Tris-buffered saline, 0.1% Tween 20 (TBST) and incubated with anti-rabbit (RRID:AB_631746; Santa Cruz Biotechnology, In, 1:5,000), anti-mouse (RRID:AB_2687626; Santa Cruz Biotechnology, In, 1:5,000) or anti-goat (RRID:AB_628490; Santa Cruz Biotechnology, In, 1:2000) horseradish peroxidase-linked immunoglobulin G for 2 hr at room temperature, and the membranes were washed several times with TBST. Immunoreactivity was detected using an enhanced chemiluminescence system (Cat. No. ELLUF0100; Merck). The intensity of each band was quantified using ImageJ software (https://imagej.nih.gov/ij/, RRID:SCR_003070).

## 2.5 | Differential expression analysis of published microarray studies

Microarray expression profiles and associated platform data were downloaded from the Gene Expression Omnibus (GEO) database for three studies: GSE49329, GSE102482, and GSE122815 using the 'GEOquery' Bioconductor package (Davis & Meltzer, 2007). Specific information regarding sample treatment and preparation can be found at the respective GEO accession numbers. Differentially expressed genes between control and LPS-treated cells or mice were identified using the GEO2R wrapper (https://www.ncbi.nlm.nih.gov/geo/geo2r/) around the Bioconductor package 'limma' (Ritchie et al., 2015). *p*-values were adjusted to correct for false positives using the Benjamini-Hochberg method. Plots of NAD-related genes were generated using GraphPad Prism v8.

## 2.6 | Immunohistochemistry

Mice were anesthetized with isoflurane and transcardially perfused with PBS followed by 4% paraformaldehyde (PFA). Brains were removed from mice and subjected to post-fixation in 4% PFA, followed by dehydration in 30% sucrose. Twenty micrometer-thick sections from −1.70 mm to −2.30 mm bregma were obtained using a cryostat (RRID:SCR_018061; Leica). To measure glial and neuronal cell loss in the mouse hippocampus sections were processed for immunostaining with antibodies against GFAP (1:1,000), Iba1 (1:500), and neurofilament H non-phosphorylated (SMI-32) (RRID:AB_2564642; BioLegend, 1:500), MAP2 (RRID:AB_10693782; Cell Signaling

Technology, 1:500). Subsequently, alexa488- (RRID:AB_2536161; Thermo Fisher Scientific Inc.,1:200) or Cy3-conjugated secondary antibodies (RRID:AB_2307443; Jackson ImmunoResearch Laboratories, Inc., 1:200) were used to visualize immunolabeling. Cell nuclei were visualized with DAPI (RRID:AB_2336790; Vector Laboratories, 1:5,000). Fluorescence images in the CA1 or CA3 of the hippocampus were obtained from 2 sections per mouse using a laser scanning confocal microscope EZ-C1 (Eclipse TE2000 U; Nikon). The fluorescence intensity of each region of the hippocampus/total area was analyzed using ImageJ software.

## 2.7 | Analysis of $NAD^+$ levels in brain tissues

After administration of apigenin or NR for 7 days, hippocampal tissues were harvested from WT mice, and $NAD^+$ levels were measured with a commercially available $NAD^+$ /NADH assay kit (Cat. No. E2ND-100; BioAssay System) according to the manufacturer's protocol. The absorbance at 570 nm for each sample was measured using a Multiskan GO Microplate Spectrophotometer (Thermo Fischer Scientific).

## 2.8 | Glial cell cultures

Astrocyte and microglial cultures were prepared from mixed glial cultures as previously described (Roboon et al., 2019). In brief, mixed glial cells were harvested from the cerebral cortices of WT neonatal mice (P1 to P3). After 14 days of cultivation, cells were collected and incubated with CD11b MicroBeads (Cat. No. 130-093-634, microbeads conjugated to monoclonal anti-human/mouse CD11b antibody, Miltenyi Biotec, Bergisch Gladbach) and applied to a magnetic column fitted into a MidiMACS™ cell separator (Cat. No. 130-042-302; Miltenyi Biotec). The cells were separated into CD11b-positive and CD11b-negative fractions. The CD11b-positive fraction, which contained microglia, was used for the experiments 24 hr after plating. The CD11b-negative fraction, which contained astrocytes, was plated and used for experiments after reaching confluence.

## 2.9 | NF-κB nuclear translocation

Cultured microglia were plated in eight chamber slides and treated with CD38 apigenin, $NAD^+$, and NR for 4 hr followed by LPS stimulation for 1 hr. Cells were then fixed with 4% PFA containing 0.2% NP-40. Cells were processed for immunocytochemistry experiments with antibodies against Iba1 and p65 (RRID:AB_10859369; Cell Signaling Technology, 1:200). Cell nuclei were visualized with DAPI (Vector Laboratories). Immunohistochemical labeling was visualized with Alexa Fluor™ 488- (RRID:AB_143165; Thermo Fisher Scientific Inc., 1:200) or Cy3- (RRID:AB_2307351, Jackson ImmunoResearch Laboratories, Inc., 1:200) conjugated secondary antibodies, and images were obtained using a laser scanning confocal microscope

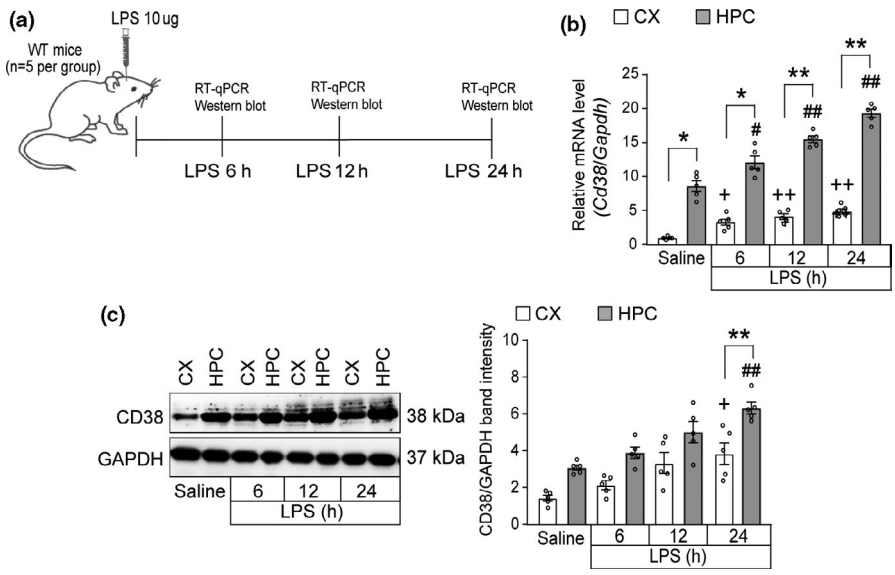


**FIGURE 1** CD38 expression was increased after LPS injection. (a) The treatment scheme and timeline of analysis. (b) RT-qPCR analysis for the expression levels of *Cd38* mRNA in the cortex (CX) and hippocampus (HPC) 6, 12, 24 hr after LPS injection. The results are expressed as fold-change relative to saline-injected mice at 6 hr. $n = 5$ mice per group. Data represent means ± *SEM*. $p$ values are determined by two-way ANOVA followed by Scheffe's $F$ test (Table 1). $^{+}p < .05$ and $^{++}p < .01$ versus saline in the CX. $^{\#}p < .05$ and $^{\#\#}p < .01$ versus saline in the HPC. $^{*}p < .05$ and $^{**}p < .01$ between the CX and HPC. (c) Western blotting analysis with antibodies against CD38 and glyceraldehyde 3-phosphate dehydrogenase (GAPDH) in the CX and HPC at different time point after LPS injection. The graph depicts the relative optical density of CD38 normalized to GAPDH. $n = 5$ mice per group. Data represent means ± *SEM*. $p$ values are determined by two-way ANOVA followed by Scheffe's $F$ test (Table 1). $^{+}p < .05$ versus saline in the CX. $^{\#\#}p < .01$ versus saline in the HPC. $^{**}p < .01$ between the CX and HPC

**TABLE 1** Summary of ANOVA analysis

| Figure | Statistical analysis | Factor | Results |
|---|---|---|---|
| 1 (b) | Two-way ANOVA | | |
| | | Brain region | $F(1,28) = 658.9$, $p < .001$ |
| | | LPS | $F(3,28) = 203.4$, $p < .001$ |
| | | Brain region with LPS | $F(3,28) = 12.9$, $p < .001$ |
| 1 (c) | two-way ANOVA | | |
| | | Brain region | $F(1,32) = 60.8$, $p < .001$ |
| | | LPS | $F(3,32) = 21.8$, $p < .001$ |
| | | Brain region with LPS | $F(3,32) = 1.39$, $p = .26$ |
| 2 (b–g) | Two-way ANOVA | | |
| | *Il1b* | Strain | $F(1,32) = 126.3$, $p < .001$ |
| | | LPS | $F(3,32) = 59.6$, $p < .001$ |
| | | Strain with LPS | $F(3,32) = 17.5$, $p < .001$ |
| | *Il6* | Strain | $F(1,32) = 17.5$, $p < .001$ |
| | | LPS | $F(3,32) = 20.3$, $p < .001$ |
| | | Strain with LPS | $F(3,32) = 4.45$, $p = .001$ |
| | *Tnf* | Strain | $F(1,32) = 16.3$, $p < .001$ |
| | | LPS | $F(3,32) = 17.2$, $p < .001$ |
| | | Strain with LPS | $F(3,32) = 4.01$, $p = .002$ |
| | *Nos2* | Strain | $F(1,32) = 32.5$, $p < .001$ |
| | | LPS | $F(3,32) = 19.6$, $p < .001$ |
| | | Strain with LPS | $F(3,32) = 6.15$, $p = .002$ |
| | *Ccl2* | Strain | $F(1,32) = 48.3$, $p < .001$ |
| | | LPS | $F(3,32) = 29.1$, $p < .001$ |
| | | Strain with LPS | $F(3,32) = 8.13$, $p < .001$ |
| | *Ccl3* | Strain | $F(1,32) = 134.1$, $p < .001$ |
| | | LPS | $F(3,32) = 61.0$, $p < .001$ |
| | | Strain with LPS | $F(3,32) = 26.1$, $p < .001$ |
| 3 (a) | Two-way ANOVA | | |
| | *Gfap* | Strain | $F(1,32) = 14.8$, $p < .001$ |
| | | LPS | $F(3,32) = 56.4$, $p < .001$ |
| | | Strain with LPS | $F(3,32) = 6.9$, $p < .001$ |
| | *Iba1* | Strain | $F(1,32) = 7.4$, $p = .010$ |
| | | LPS | $F(3,32) = 26.3$, $p < .001$ |
| | | Strain with LPS | $F(3,32) = 3.7$, $p = .022$ |
| 3 (b–c) | Two-way ANOVA | | |
| | GFAP in CA1 | Strain | $F(1,16) = 14.1$, $p = .001$ |
| | | LPS | $F(1,16) = 91.3$, $p < .001$ |
| | | Strain with LPS | $F(1,16) = 11.5$, $p = .003$ |
| | GFAP in CA3 | Strain | $F(1,16) = 79.1$, $p < .001$ |
| | | LPS | $F(1,16) = 317.4$, $p < .001$ |
| | | Strain with LPS | $F(1,16) = 96.5$, $p < .001$ |
| | Iba1 in CA1 | Strain | $F(1,16) = 16.8$, $p < .001$ |
| | | LPS | $F(1,16) = 137.1$, $p < .001$ |
| | | Strain with LPS | $F(1,16) = 16.9$, $p < .001$ |
| | Iba1 in CA3 | STRAIN | $F(1,16) = 8.0$, $p = .012$ |

(Continues)

**TABLE 1** (Continued)

| Figure | Statistical analysis | Factor | Results |
|---|---|---|---|
| | | LPS | $F(1,16) = 46.6$, $p < .001$ |
| | | Strain with LPS | $F(1,16) = 5.3$, $p = .035$ |
| 4 (b) | One-way ANOVA | | |
| | | Treatment | $F(2,15) = 15.7$, $p < .001$ |
| 4 (c–e) | Two-way ANOVA | | |
| | *Il1b* | Treatment | $F(2,27) = 4.65$, $p = .018$ |
| | | LPS | $F(1,27) = 49.7$, $p < .001$ |
| | | Treatment with LPS | $F(2,27) = 4.05$, $p = .028$ |
| | *Il6* | Treatment | $F(2,27) = 8.11$, $p = .002$ |
| | | LPS | $F(1,27) = 97.0$, $p < .001$ |
| | | Treatment with LPS | $F(2,27) = 8.70$, $p = .001$ |
| | *Tnf* | Treatment | $F(2,27) = 7.61$, $p = .002$ |
| | | LPS | $F(1,27) = 50.1$, $p < .001$ |
| | | Treatment with LPS | $F(2,27) = 6.42$, $p = .005$ |
| 4 (g) | Two-way ANOVA | | |
| | | Strain | $F(3,32) = 13.6$, $p < .001$ |
| | | Treatment | $F(1,32) = 337.6$, $p < .001$ |
| | | Strain with treatment | $F(3,32) = 1.94$, $p = .142$ |
| 4 (h–j) | Two-way ANOVA | | |
| | *Il1b* | Strain | $F(3,32) = 36.5$, $p < .001$ |
| | | Treatment | $F(1,32) = 31.4$, $p < .001$ |
| | | Strain with treatment | $F(3,32) = 8.7$, $p < .001$ |
| | *Il6* | Strain | $F(3,32) = 22.1$, $p < .001$ |
| | | Treatment | $F(1,32) = 7.2$, $p = .011$ |
| | | Strain with treatment | $F(3,32) = 4.1$, $p = .013$ |
| | *Tnf* | Strain | $F(3,32) = 39.5$, $p < .001$ |
| | | Treatment | $F(1,32) = 7.2$, $p < .001$ |
| | | Strain with treatment | $F(3,32) = 4.3$, $p = .011$ |
| 4 (l) | One-way ANOVA | | |
| | | Treatment | $F(5,18) = 217.9$, $p < .001$ |
| 4 (m–o) | One-way ANOVA | | |
| | *Il1b* | Treatment | $F(5,18) = 18.9$, $p < .001$ |
| | *Il6* | Treatment | $F(5,18) = 51.7$, $p < .001$ |
| | *Tnf* | Treatment | $F(5,18) = 22.1$, $p < .001$ |
| 5 (b–d) | two-way ANOVA | | |
| | GFAP in CA1 | Treatment | $F(2,21) = 6.4$, $p = .006$ |
| | | LPS | $F(1,21) = 73.4$, $p < .001$ |
| | | Treatment with LPS | $F(2,21) = 13.1$, $p < .001$ |
| | GFAP in CA3 | Treatment | $F(2,20) = 26.1$, $p < .001$ |
| | | LPS | $F(1,20) = 117.9$, $p < .001$ |
| | | Treatment with LPS | $F(2,20) = 44.0$, $p < .001$ |
| | Iba1 in CA1 | Treatment | $F(2,21) = 7.24$, $p = .004$ |
| | | LPS | $F(1,21) = 211.3$, $p < .001$ |
| | | Treatment with LPS | $F(2,21) = 8.78$, $p = .002$ |
| | Iba1 in CA3 | treatment | $F(2,21) = 10.3$, $p < .001$ |

(Continues)

**TABLE 1** (Continued)

| Figure | Statistical analysis | Factor | Results |
|---|---|---|---|
| | | LPS | $F(1,21) = 67.9$, $p < .001$ |
| | | Treatment with LPS | $F(2,21) = 5.2$, $p = .014$ |
| 6 (b–c) | Two-way ANOVA | | |
| | SMI32 in CA1 | Treatment | $F(2,24) = 3.5$, $p = .045$ |
| | | LPS | $F(1,24) = 38.9$, $p < .001$ |
| | | Treatment with LPS | $F(2,24) = 2.7$, $p = .085$ |
| | SMI32 in CA3 | Treatment | $F(2,24) = 13.7$, $p < .001$ |
| | | LPS | $F(1,24) = 150.0$, $p < .001$ |
| | | Treatment with LPS | $F(2,24) = 7.6$, $p = .002$ |
| | MAP2 in CA1 | Treatment | $F(2,24) = 3.6$, $p = .041$ |
| | | LPS | $F(1,24) = 50.2$, $p < .001$ |
| | | Treatment with LPS | $F(2,24) = 5.1$, $p = .014$ |
| | MAP2 in CA3 | Treatment | $F(2,24) = 10.4$, $p < .001$ |
| | | LPS | $F(1,24) = 7.5$, $p = .011$ |
| | | Treatment with LPS | $F(2,24) = 0.5$, $p = .622$ |
| 7 (a–d) | Two-way ANOVA | | |
| | *Il1b* | Treatment | $F(4,40) = 7.3$, $p < .001$ |
| | | LPS | $F(1,40) = 281.3$, $p < .001$ |
| | | Treatment with LPS | $F(4,40) = 7.2$, $p < .001$ |
| | *Il6* | Treatment | $F(4,40) = 5.3$, $p = .001$ |
| | | LPS | $F(1,40) = 81.6$, $p < .001$ |
| | | Treatment with LPS | $F(4,40) = 5.4$, $p = .001$ |
| | *Tnf* | Treatment | $F(4,40) = 6.7$, $p < .001$ |
| | | LPS | $F(1,40) = 140.7$, $p < .001$ |
| | | Treatment with LPS | $F(4,40) = 6.7$, $p < .001$ |
| | *Nos2* | Treatment | $F(4,40) = 3.6$, $p < .013$ |
| | | LPS | $F(1,40) = 61.0$, $p < .001$ |
| | | Treatment with LPS | $F(4,40) = 3.7$, $p = .012$ |
| 7 (e–h) | Two-way ANOVA | | |
| | *Il1b* | Treatment | $F(4,40) = 7.3$, $p < .001$ |
| | | LPS | $F(1,40) = 281.3$, $p < .001$ |
| | | Treatment with LPS | $F(4,40) = 7.2$, $p < .001$ |
| | *Il6* | Treatment | $F(4,40) = 5.3$, $p = .001$ |
| | | LPS | $F(1,40) = 81.6$, $p < .001$ |
| | | Treatment with LPS | $F(4,40) = 5.4$, $p = .001$ |
| | *Tnf* | Treatment | $F(4,40) = 6.7$, $p < .001$ |
| | | LPS | $F(1,40) = 140.7$, $p < .001$ |
| | | Treatment with LPS | $F(4,40) = 6.7$, $p < .001$ |
| | *Nos2* | Treatment | $F(4,40) = 3.6$, $p < .013$ |
| | | LPS | $F(1,40) = 61.0$, $p < .001$ |
| | | Treatment with LPS | $F(4,40) = 3.7$, $p = .012$ |
| 8 (b) | Two-way ANOVA | | |
| | | Treatment | $F(4,390) = 37.4$, $p < .001$ |
| | | LPS | $F(1,390) = 1,342.6$, $p < .001$ |
| | | Treatment with LPS | $F(4,390) = 35.1$, $p < .001$ |

EZ-C1. The nuclear fluorescence intensity of p65 was determined by Integrated Density − (Area of selected cell × mean fluorescence of background) using ImageJ software.

### 2.10 | Statistical analysis

All statistical analyses were performed using Statcel Ver.3 (OMS Publishing Inc.). The experimental results are expressed as mean ± standard error of the mean (*SEM*), with the number of experiments indicated by 'n'. No statistical evaluations were performed to predetermine sample size, but our sample sizes were similar to those generally used in the field. Since a Shapiro–Wilk test showed normal distribution of all data sets in this study, a parametric analysis of variance (ANOVA) was applied to test for statistical differences of the means. One-way ANOVA followed by the Tukey–Kramer test or two-way ANOVA followed by Scheffe's *F* test was used for the statistical analysis. *p* values <.05 were considered statistically significant. No statistical test for outliners was conducted and no data point was excluded.

## 3 | RESULTS

### 3.1 | CD38 expression was increased after LPS injection

We first investigated the expression of CD38 in LPS-induced neuroinflammation by RT-qPCR and Western blot analysis. Tissue samples were collected at 6, 12, and 24 hr after intracerebroventricular (i.c.v.) injection of LPS (Figure 1a). Consistent with our recent report in the cuprizone-induced demyelinating model (Roboon et al., 2019), RT-qPCR analysis revealed that the expression of *Cd38* mRNA gradually increased in both the cerebral cortex and hippocampus, and reached significance after 6 hr of LPS injection. Furthermore, the level of *Cd38* mRNA expression was higher in the hippocampus than in the cerebral cortex at any time point after LPS injection (Figure 1b; for results of ANOVA analysis, see Table 1). Western blot analysis confirmed the gradual increase in CD38 protein expression after LPS injection. The expression level of CD38 protein was also higher in the hippocampus than in the cerebral cortex (Figure 1c and Table 1). Furthermore, analysis of microarray data also showed elevated expression levels of CD38 mRNA in the brain after LPS injection and in the primary microglia after LPS stimulation (Figure S1). Interestingly, we found that other $NAD^+$-consuming enzymes, PARPs (poly (ADP-ribose) polymerases), were also significantly increased by induction of neuroinflammation (Figure S1). These results suggest that CD38 and other NAD-consuming molecules may be involved in LPS-induced neuroinflammation.

### 3.2 | LPS-induced neuroinflammation and glial activation were attenuated in CD38 KO mice

To evaluate the effect of CD38 deletion on LPS-induced neuroinflammation and glial activation, we analyzed the expression of pro-inflammatory genes and glia-associated genes after LPS injection by RT-qPCR, Western blot analysis and immunohistochemistry. Tissues were collected at 6, 12, and 24 hr after LPS injection (Figure 2a). RT-qPCR analysis revealed that the expression of genes such as *Il1b*, *Il6*, *Tnf*, *Nos2*, *Ccl2*, and *Ccl3* was robustly increased in WT mice 6 hr after LPS injection (Figure 2b–g). In all cases except *Il1b*, mRNA expression

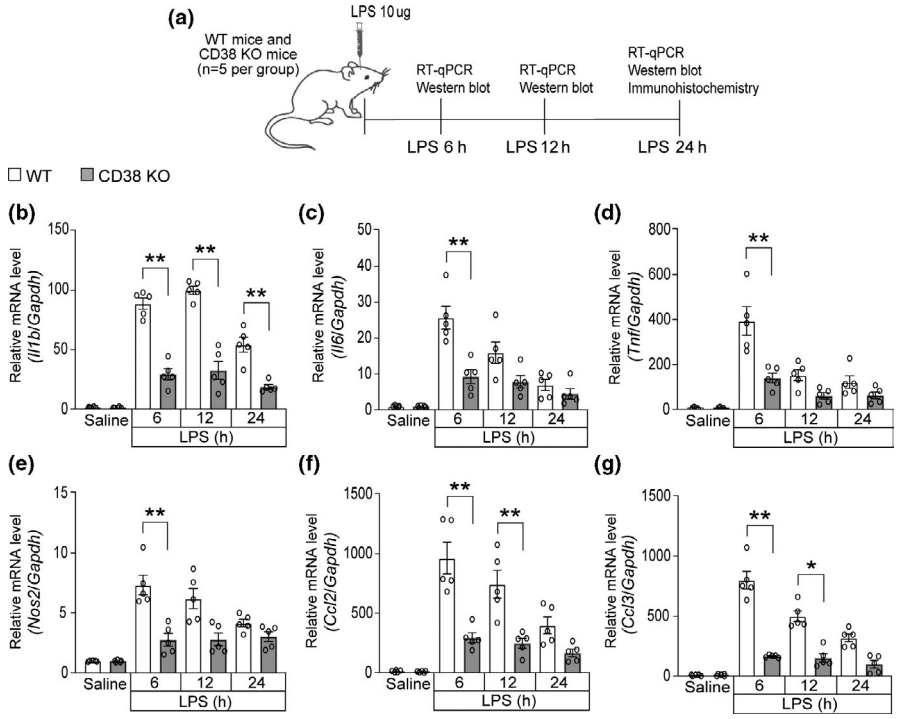


**FIGURE 2** LPS-induced neuroinflammation was attenuated in CD38 KO mice. (a) The treatment scheme and timeline of analysis. (b–g) RT-qPCR analysis for the expression of inflammatory genes in the HPC 6, 12, 24 hr after LPS injection in WT and CD38 KO mice. The results are expressed as fold-change relative to saline-injected WT mice at 6 hr. $n = 5$ mice per group. Data represent means ± *SEM*. *p* values are determined by two-way ANOVA followed by Scheffe's *F* test (Table 1). $^*p < .05$ and $^{**}p < .01$ between WT and CD38 KO mice

reached a peak 6 hr after LPS injection and gradually decreased thereafter (Figure 2c–g). The expression of these genes was significantly lower in CD38 KO mice than in WT mice (Figure 2b–g and Table 1). The expression of mRNAs for *Gfap* and *Iba1*, an astrocytic and microglial marker, respectively, gradually increased and reached significantly high levels at 12 hr and 24 hr, respectively, after LPS injection in WT mice (Figure 3a and Table 1). Expression of *Gfap* and *Iba1* was significantly lower in CD38 KO mice. Immunohistochemical analysis further revealed that the immunoreactivity of GFAP and Iba1 was clearly increased in both the CA1 and CA3 regions of the hippocampus 24 hr after LPS injection, but the level was significantly lower in CD38 KO mice (Figure 3b,c and Table 1). These data indicate that deletion of CD38 suppresses LPS-induced neuroinflammation and glial activation.

### 3.3 | NR and apigenin ameliorated LPS-induced neuroinflammation and glial activation

The phenotypes in CD38 KO mice described above and our recent study (Roboon et al., 2019) suggest that pharmacological inhibition of CD38 and/or boosted brain $NAD^+$ level may be capable of depressing pathological inflammation in neurological diseases. Therefore, we assessed the effect of apigenin, a natural flavonoid

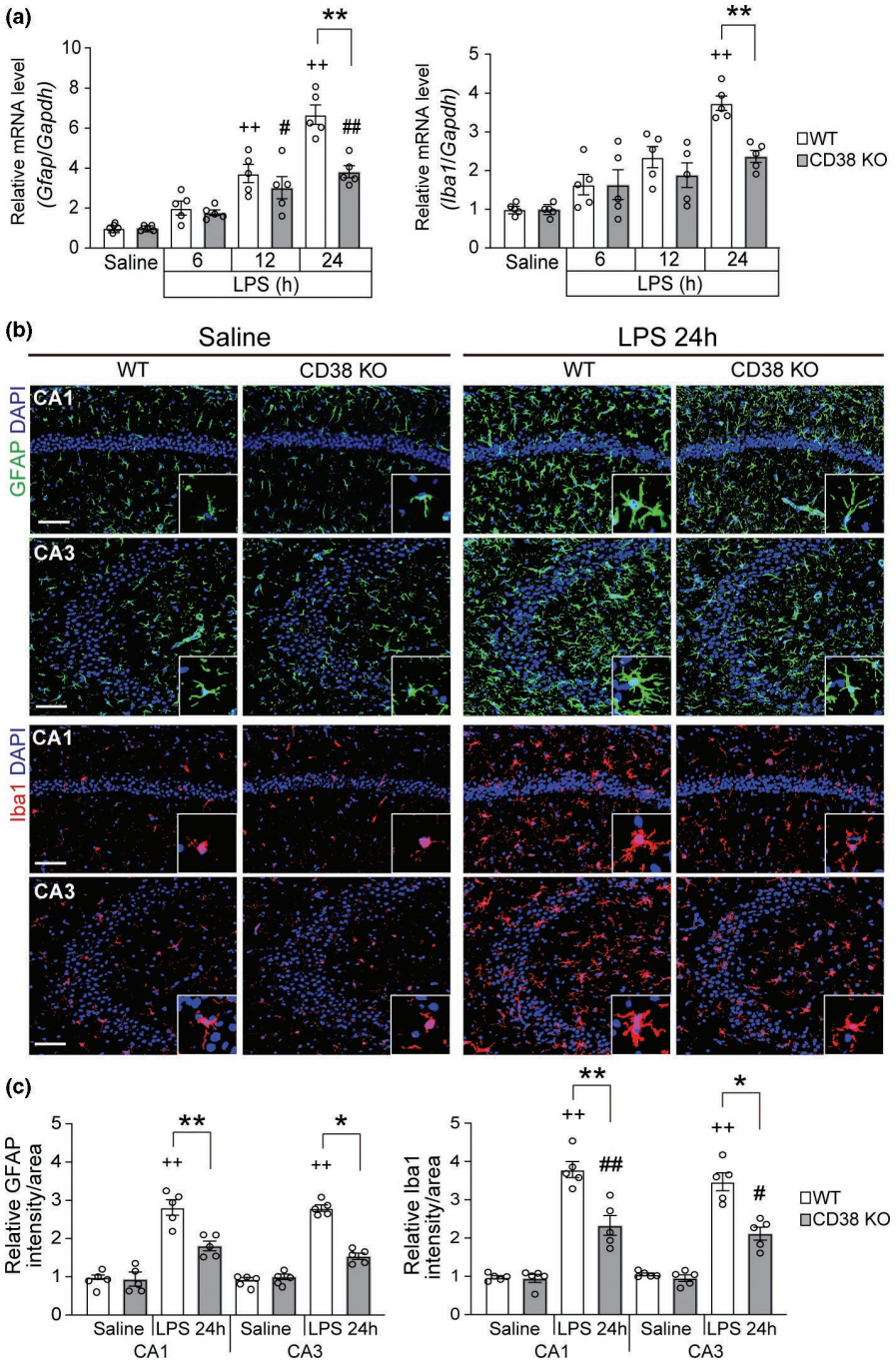


**FIGURE 3** LPS-induced glial activation was attenuated in CD38 KO mice. (a) RT-qPCR analysis for expression levels of *Gfap* and *Iba1* mRNA in the HPC of WT and CD38 KO mice 6, 12, 24 hr after LPS injection. The results are expressed as fold-change relative to saline-injected WT mice at 6 hr. $n = 5$ mice per group. (b) Representative immunofluorescence images of GFAP (green) and Iba1 (red) of 24 hr after saline or LPS injection in the HPC (CA1 and CA3) of WT and CD38 KO mice. Nuclei were counterstained with DAPI. Scale bars: 100 μm. (c) The graphs represent the intensity of GFAP (left) and Iba1 (right) 24 hr after saline or LPS injection in the CA1 and CA3 of WT and CD38 KO mice. The results are expressed as fold-change relative to saline-injected WT mice at 24 hr. $n = 5$ mice per group. Data represent means ± *SEM*. *p* values are determined by two-way ANOVA followed by Scheffe's *F* test (Table 1). $^{+}p < .05$ and $^{++}p < .01$ versus 0 hr of LPS in the WT mice. $^{\#}p < .05$ and $^{\#\#}p < .01$ versus 0 hr of LPS in the CD38 KO mice. $^{*}p < .05$ and $^{**}p < .01$ between WT and CD38 KO mice

that acts as a CD38 inhibitor (Escande et al., 2013), and NR, an $NAD^+$ precursor (Bieganowski & Brenner, 2004), on $NAD^+$ levels in the context of LPS-injected neuroinflammation. Apigenin or NR was administered intraperitoneally once per day for seven consecutive days, followed by LPS injection 6 hr after the final administration of apigenin or NR. Tissues for $NAD^+$ measurement and RT-qPCR were collected 6 hr after the last administration and 6 hr after LPS injection, respectively (Figure 4a). The $NAD^+$ levels in the hippocampus were significantly higher in apigenin- or NR-administered mice than in control mice, and the levels were similar in both conditions (Figure 4b and Table 1). WT mice were pre-administered with apigenin or NR for 7 days, and then injected with LPS 6 hr after the final administration of each compound. RT-qPCR analysis revealed that the induction of inflammatory genes such as *Il1b*, *Il6* and *Tnf* was suppressed in compound-pre-administered mice than in control mice (Figure 4c–e and Table 1). Furthermore, we examined $NAD^+$ levels and neuroinflammation in CD38 KO mice administered NR or apigenin. Tissues were collected 6 hr after LPS injection (Figure 4f). Although CD38 KO mice showed significantly higher $NAD^+$ levels than WT mice in any group, there was not further increase of $NAD^+$ by NR or apigenin in CD38 KO mice (Figure 4g and Table 1). Consistent with CD38 as the target of apigenin, apigenin did not increase the elevated $NAD^+$ level in CD38 KO mice. Additionally, CD38 KO mice exhibited lower expression of proinflammatory genes as shown in Figure 2, and apigenin or NR did not further decrease these gene expression programs (Figure 4h–j and Table 1). To assess whether boosting $NAD^+$ prior to LPS-induced neuroinflammation is important or not, apigenin or NR was administered once immediately after LPS injection. Tissues are collected 6 hr after LPS injection (Figure 4k).

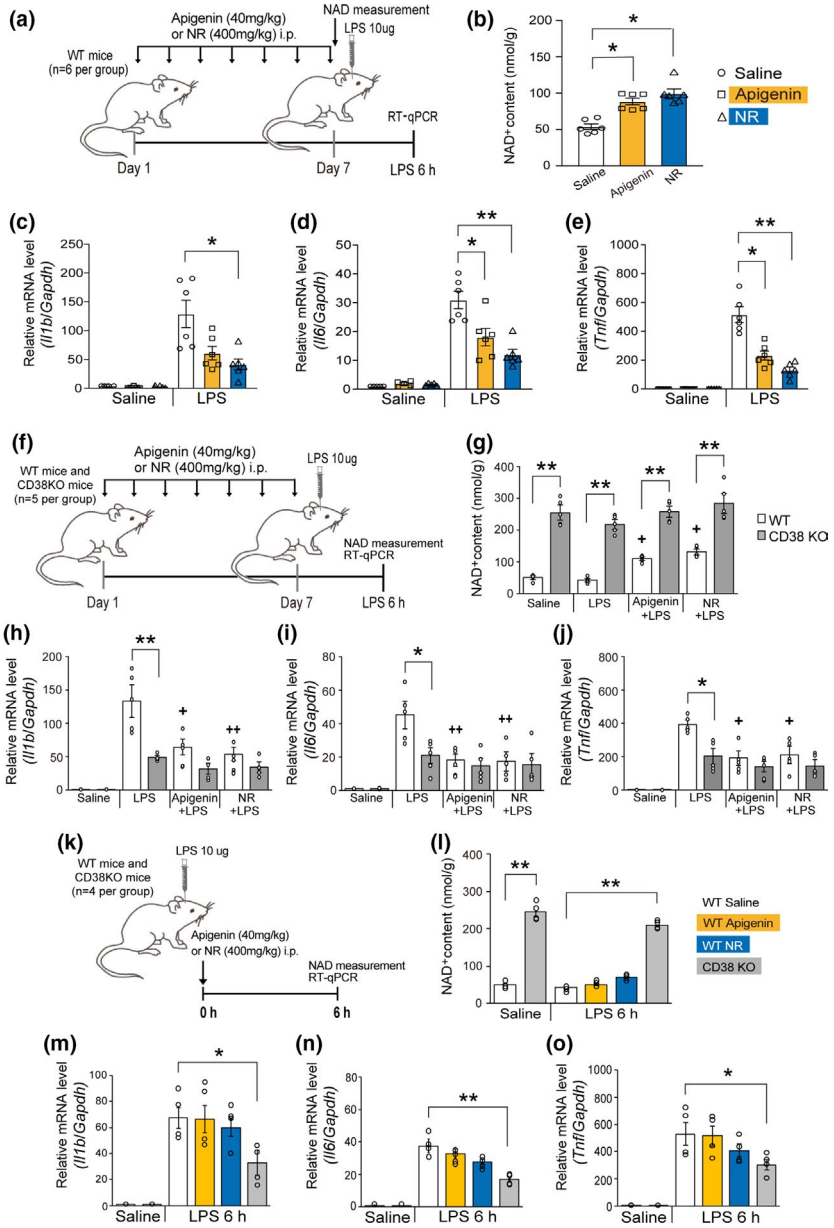

**FIGURE 4** NR and apigenin ameliorated LPS-induced neuroinflammation. (a, f, k) The treatment scheme and timeline of analysis. (b) $NAD^+$ levels in the HPC of WT mice were evaluated 6 hr after the last treatment with saline, apigenin 40 mg/kg or NR 400 mg/kg via i.p. injection for 7 days. $n = 6$ mice per group. Data represent means ± *SEM*. *p* values are determined by one-way ANOVA followed Tukey–Kramer test (Table 1). $^*p < .05$ compared saline. (c–e) RT-qPCR analysis for the expression of inflammatory genes in the HPC of saline- or LPS injected-WT mice pretreated with saline, apigenin or NR for 7 days. The results are expressed as fold-change relative to saline-injected WT mice pretreated with saline. $n = 6$ mice per group. Data represent means ± *SEM*. *p* values are determined by two-way ANOVA followed by Scheffe's *F* test (Table 1). $^*p < .05$ and $^{**}p < .01$ versus LPS-injected mice pretreated with saline. (g) Saline, apigenin 40 mg/kg or NR 400 mg/kg was administered via i.p. injection for 7 days. $NAD^+$ was measured 6 hr after LPS injection. $n = 5$ mice per group. Data represent mean ± *SEM*. *p* values were determined by two-way ANOVA followed by Scheffe's *F* test (Table 1). $^{**}p < .01$ between WT and CD38 KO mice and $^{+}p < .05$ versus. saline-injected WT mice. (h–j) RT-qPCR analysis for the expression of inflammatory genes in the HPC of saline- or LPS-injected WT and CD38 KO mice pretreated with saline, apigenin, or NR for 7 days in WT and CD38 KO mice. The results are expressed as fold-change relative to saline-injected WT mice pretreated with saline. $n = 5$ mice per group. Data represent mean ± *SEM*. *P* values were determined by two-way ANOVA followed by Scheffe's *F* test (Table 1). $^*p < .05$ and $^{**}p < .01$ between WT and CD38 KO mice. $^{+}p < .05$, $^{++}p < .01$ versus. LPS-injected WT mice. (l) Single-dose of saline, apigenin 40 mg/kg or NR 400 mg/kg was administered via i.p. injection immediately after LPS injection. $NAD^+$ was measured 6 hr after LPS injection. $n = 4$ mice per group. Data represent means ± *SEM*. *p* values are determined by one-way ANOVA followed Tukey–Kramer test (Table 1). $^{**}p < .01$ compared to WT saline. (m-o) RT-qPCR analysis for the expression of inflammatory genes in the HPC of saline- or LPS injected-WT or -CD38 KO mice treated with saline, apigenin or NR. The results are expressed as fold-change relative to saline-injected WT mice treated with saline. $n = 4$ mice per group. Data represent means ± *SEM*. *p* values are determined by one-way ANOVA followed Tukey–Kramer test (Table 1). $^*p < .05$ and $^{**}p < .01$ versus LPS-injected mice treated with saline

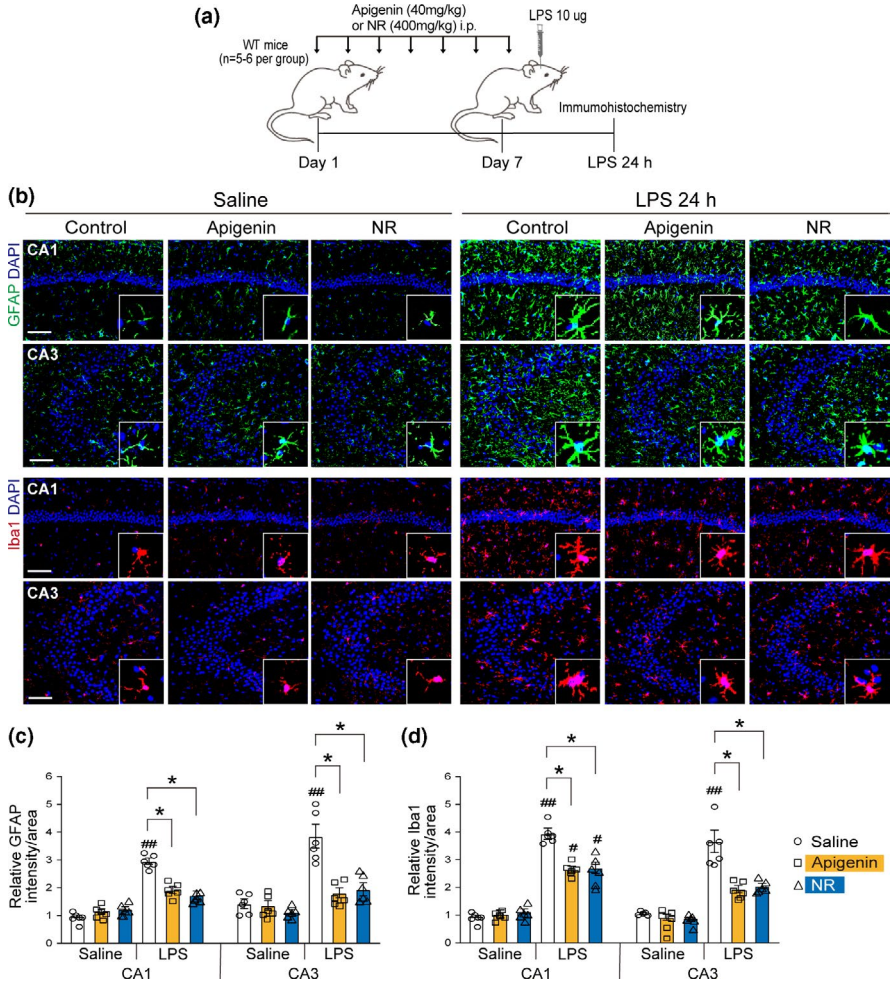


**FIGURE 5** NR and apigenin ameliorated LPS-induced glial activation. (a) The treatment scheme and timeline of analysis. (b) Representative immunofluorescence images of GFAP (green) and Iba1 (red) 24 hr after saline or LPS injection in the HPC (CA1 and CA3) of WT mice pretreated with saline, apigenin or NR for 7 days. Nuclei were counterstained with DAPI. Scale bars: 100 μm. (c) The graphs represent the intensity of GFAP and Iba1 in the HPC (CA1 and CA3). The results are expressed as fold-change relative to saline-injected WT mice pretreated with saline. $n = 6$ mice per group. Data represent means ± *SEM*. *p* values are determined by two-way ANOVA followed by Scheffe's *F* test (Table 1). $^*p < .05$ versus LPS-injected mice pretreated with saline. $^{\#\#}p < .01$ between saline- and LPS-injected mice

Single-dose administration of apigenin did not increased $NAD^+$ level. NR slightly, but not significantly, increased $NAD^+$ level. However, the level was much lower than that of CD38 KO mice (Figure 4l and Table 1). Correlated with these $NAD^+$ levels, NR had weak suppressive effect on expression of inflammatory genes compared with that of CD38 KO mice (Figure 4m–o and Table 1).

To assess the effect of apigenin and NR on glial activation, these compounds were pre-administered intraperitoneally once per day

for 7 consecutive days, followed by LPS injection. Brains were fixed 24 hr after LPS injection (Figure 5a). Immunohistochemical analysis revealed enhanced levels of immunoreactivity for GFAP and Iba1 24 hr after LPS injection, but levels were reduced in apigenin or NR pre-administered mice compared to the control group of mice (Figure 5b–d and Table 1). These results suggest that the levels of CD38 and $NAD^+$ determine the state of neuroinflammation and the activation of both astrocytes and microglia in the brain.

### 3.4 | NR and apigenin attenuated LPS-induced neurodegeneration

As LPS-induced neuroinflammation often leads to neurodegeneration (Deng et al., 2014; Pintado et al., 2012; Qin et al., 2007; Wang et al., 2019), the effect of apigenin and NR on neuronal damage was evaluated after LPS injection. Immunohistochemistry for non-phosphorylated neurofilament H (SMI32), a marker of damaged axons, revealed that neurodegeneration occurred within 24 hr after LPS injection in both the CA1 and CA3 regions of the hippocampus, and the level was significantly lower in apigenin or NR pre-administered mice (Figure 6a,b and Table 1). Consistent with these results, immunohistochemistry for MAP2 revealed that the intensity of normal axons and dendrites decreased after LPS injection, and this decrease was partially recovered by apigenin or NR pre-administration (Figure 6a,c and Table 1). These results suggest that administration of NR or apigenin attenuated not only LPS-induced neuroinflammation but also subsequent LPS-induced neurodegeneration.

### 3.5 | NR, apigenin, and 78c reduced inflammatory response in vitro

Silencing of *the cd38* gene and the addition of $NAD^+$ suppressed LPS-induced activation of astrocytes and microglia in vitro (Hattori et al., 2017; Roboon et al., 2019), the effects of NR, apigenin, and 78c, the latter a CD38-specific inhibitor, on the inflammatory response were examined using cultured microglia and astrocytes. RT-qPCR analysis revealed that LPS strongly up-regulated the expression of pro-inflammatory genes, such as *Il1b*, *Il6*, *Tnf*, *Nos2* in microglia and/or astrocytes. In microglia, the expression of *Il1b* and *Il6* was significantly reduced by all compounds, and that of *Tnf* and *Nos2* was significantly decreased by $NAD^+$ and NR, and apigenin, respectively (Figure 7a–d and Table 1). In addition, in astrocytes, all compounds showed a tendency to suppress the induction of inflammatory genes, although the expression of *Il6* was significantly decreased by apigenin, and that of *Tnf* was significantly reduced by $NAD^+$ after LPS injection (Figure 7e–h and Table 1). These results suggest that inhibition of CD38 and increased $NAD^+$ status directly suppress LPS-induced inflammatory responses, especially in microglia.

### 3.6 | NR, apigenin, and 78c suppressed NF-κB signaling pathway

It is known that LPS binds to toll-like receptor 4, which activates the NF-κB cascade and consequently induces pro-inflammatory genes. To determine the relevance of CD38 inhibition and supplementation

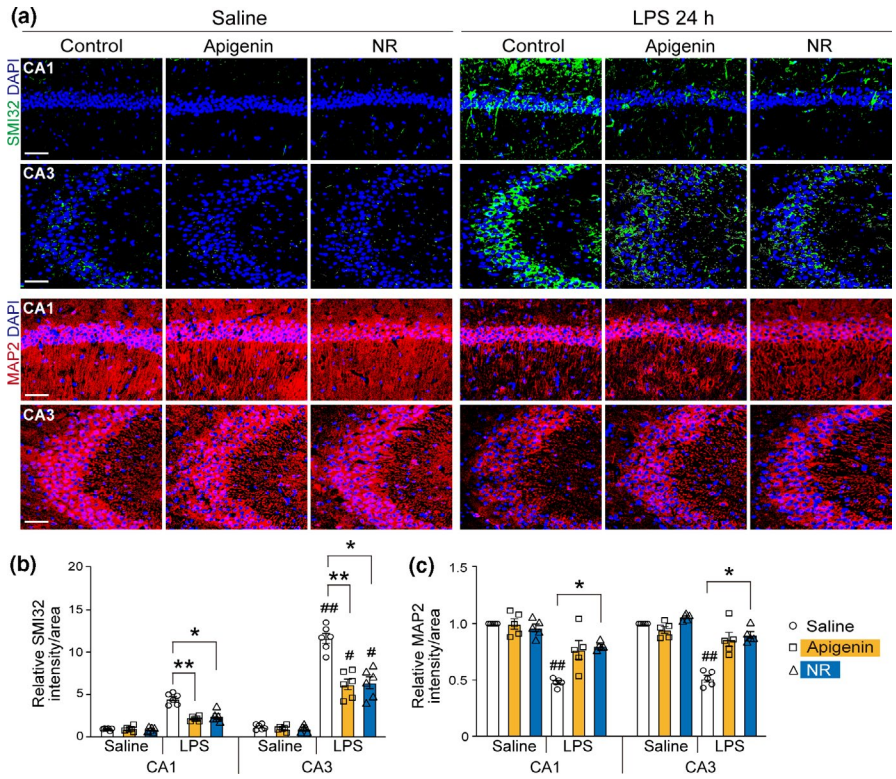


**FIGURE 6** NR and apigenin ameliorated LPS-induced neurodegeneration. (a) Representative immunofluorescence images of SMI32 and MAP2 24 hr after saline or LPS injection in the HPC (CA1 and CA3) of WT mice pretreated with saline, apigenin or NR for 7 days. Nuclei were counterstained with DAPI. Scale bars: 100 μm. (b, c) The graphs represent the intensity of SMI32 and MAP2 in the HPC (CA1 and CA3). The results are expressed as fold-change relative to saline-injected WT mice pretreated with saline. $n = 6$ mice per group. Data represent means ± *SEM*. *p* values are determined by two-way ANOVA followed by Scheffe's *F* test (Table 1). $^*p < .05$ and $^{**}p < .01$ versus LPS injected mice pretreated with saline. $^{\#}p < .05$ and $^{\#\#}p < .01$ between saline- and LPS-injected mice

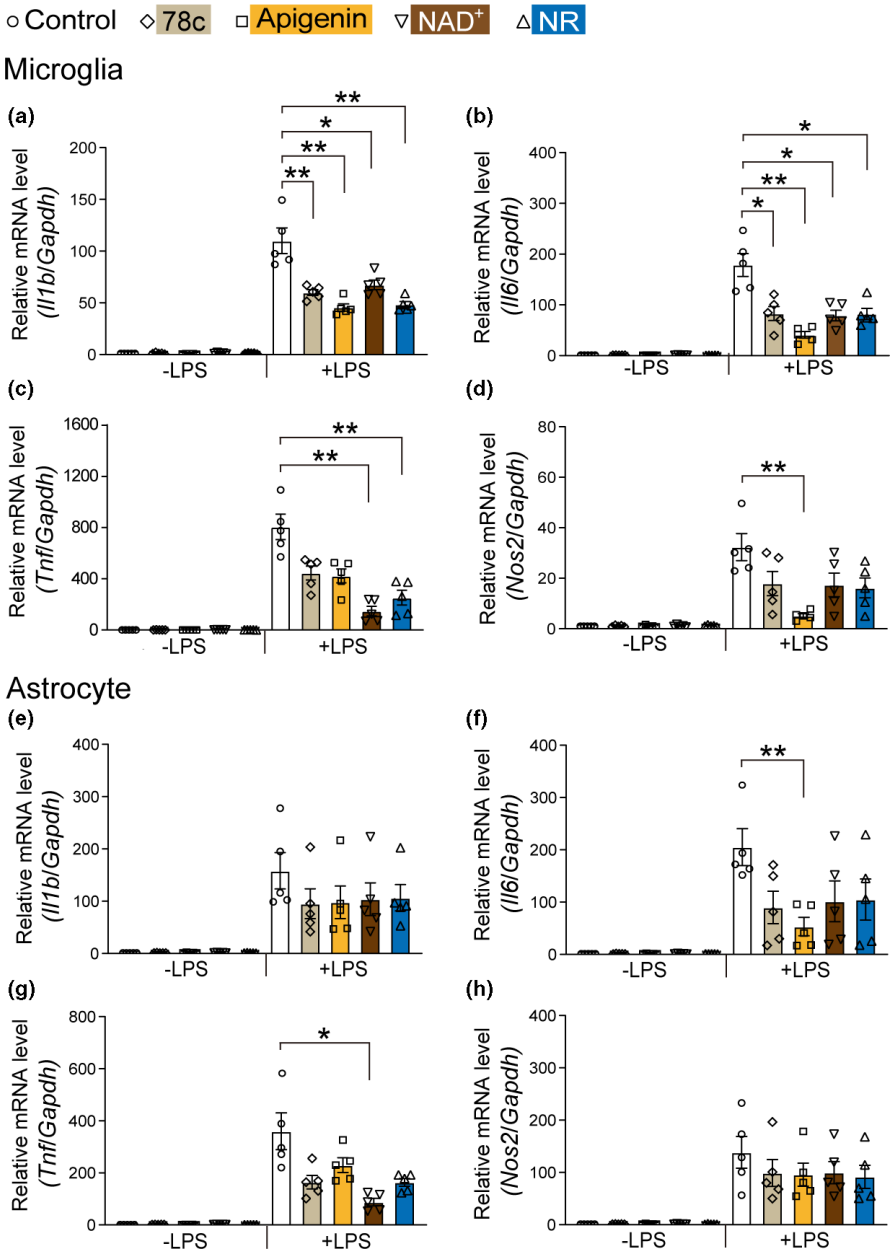


**FIGURE 7** NR, apigenin, and 78c reduced inflammatory response in vitro. RT-qPCR analysis for the expression levels of inflammatory genes in glial cultures. (a–h) Microglia (a–d) or astrocyte (e-h) cultures were treated with PBS, 78c, apigenin, $NAD^+$ or NR for 4 hr, then stimulated with LPS (100 ng/ml) for 6 hr. The results are expressed as fold-change relative to control cells without LPS. $n = 5$ of independent cell culture preparations. Data represent means ± *SEM*. *p* values are determined by two-way ANOVA followed Scheffe's *F* test (Table 1). $^*p < .05$ and $^{**}p < .01$ versus LPS-treated control cells

of $NAD^+$ in the NF-κB signaling pathway, the nuclear translocation of NF-κB was examined after LPS stimulation in cultured microglia. Immunocytochemical analysis revealed that the intensity of p65, a major component of NF-κB, in the nucleus was strongly increased 1 hr after LPS stimulation. In contrast, it was significantly reduced by all the compounds (Figure 8a,b and Table 1). NF-κB activation in astrocytes was also reduced by these compounds 1 hr after LPS stimulation (Figure S2). Furthermore, to investigate effect of $NAD^+$ on JAK/STAT signaling pathway, we examined Stat3 and p-Stat3 expression in CD38 KO mice and NR- or apigenin-administered mice after LPS injection. Although p-Stat3 was clearly increased by LPS injection, its expression was not changed by deletion of CD38 nor administration of these compounds (Figure S3). These results suggest that intracellular $NAD^+$ suppresses LPS-induced NF-κB activation.

## 4 | DISCUSSION

In the current study, we investigated the effect of CD38 inhibition and supplementation of $NAD^+$ on LPS-induced neuroinflammation in mice. CD38 expression was increased both in the hippocampus and in the cerebral cortex after LPS injection. Deletion of CD38 decreased LPS-induced neuroinflammation and glial activation Consistently, pre-administration of apigenin and NR increased $NAD^+$ concentration in the brain, and suppressed LPS-induced inflammatory response, glial activation, and neurodegeneration. In primary cultured glial cells, compounds such as 78c, apigenin, $NAD^+$, and NR effectively suppressed the activation of NF-κB and the induction of cytokines and chemokines after LPS treatment. These results suggest that boosting $NAD^+$ by CD38 inhibition and NR supplementation has suppressive effect on neuroinflammation in the brain.

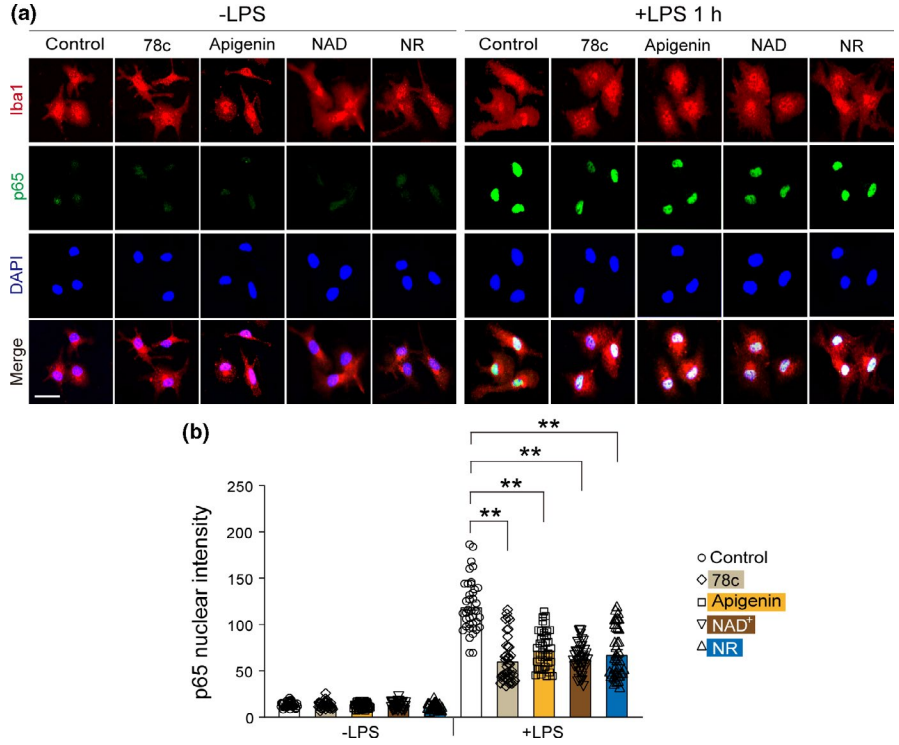


**FIGURE 8** NR, apigenin, and 78c suppressed NF-κB signaling pathway in microglia. (a) Cultured microglia were treated with PBS, 78c, apigenin, $NAD^+$ or NR for 4 hr, then stimulated with LPS (100 ng/ml) for 1 hr. After fixation, cells were subjected to immunohistochemistry of p65 and Iba1. Nuclei were counterstained with DAPI. Scale bar: 50 μm. (b) The graphs represent the intensity of p65 in the nucleus. Fifty cells per condition were analyzed, from four independent cell culture preparations. Data represent means ± *SEM*. *p* values are determined by two-way ANOVA followed by Scheffe's *F* test (Table 1). $^*p < .01$ versus LPS-treated control cells

### 4.1 | The role of $NAD^+$ AND CD38 in LPS-induced neuroinflammation

To date, several studies, including ours, have suggested the involvement of CD38 in neuroinflammation. Deletion of CD38 in the APP.PS Alzheimer's disease model exhibited a significant reduction in Aβ plaque load and microglia/macrophage accumulation in the brain compared with APP.PS mice with CD38 intact (Blacher et al., 2015). Our previous study also revealed that CD38 KO mice ameliorated demyelination, glial activation, and neuroinflammation in cuprizone-induced demyelination (Roboon et al., 2019). To explore the direct effects of CD38 deletion or inhibition, and supplementation of $NAD^+$ on neuroinflammation, we employed a mouse model of LPS-injection into the lateral cerebral ventricle in the current study. Our results demonstrated that CD38 deletion or inhibition, and supplementation with $NAD^+$ suppressed neuroinflammation at earlier stages (within 6 hr) after LPS administration in vivo (Figures 2 and 4) and in vitro (Figures 7 and 8), and these effects seem to be correlated with the increased level of $NAD^+$ in the brain (Figure 4b,g) (Roboon et al., 2019). Administration of NR did not have further suppressive effect on neuroinflammation in CD38 KO mice (Figure 4h–j). This might because CD38 KO mice had much higher $NAD^+$ levels than WT mice in any group and there was no further increase of $NAD^+$ by NR administration in CD38 KO mice (Figure 4g). Although pre-administration of apigenin or NR for 7 days significantly reduced LPS-induced neuroinflammtion, single-dose administration of these compounds simultaneously with LPS injection had no or weak effect of increasing $NAD^+$ and suppression of neuroinflammation (Figure 4). To boost $NAD^+$ level enough to mitigate neuroinflammation, multiple pre-administration of apigenin and NR seems to be necessary. Furthermore, $NAD^+$ level was not significantly decreased by LPS injection in WT mice (Figure 4l). Therefore, boosting $NAD^+$ prior to LPS-induced neuroinflammation seems to be more important than reducing depletion of $NAD^+$ after LPS injection.

The biology of inflammation suggests that expression of inflammatory markers, including CD38, cytokines, and chemokines, constitutes a homeostatic attempt at controlling infection or environmental damage. However, uncontrolled inflammatory responses are clearly neurotoxic. The behavioral deficits of mice with CD38 deletion suggest that the formation of CD38-dependent second messengers, including cADPR (Takasawa, Tohgo et al., 1993) and NAADP (Nam et al., 2020), is required for oxytocin signaling, social intelligence, and parenting (Jin et al., 2007). In the case of neuroinflammatory responses, we consider that the formation of CD38-dependent signals might induce such activities and/or elevated NAD might depress such activities.

Expression of glial markers such as GFAP and Iba1 (Figures 3 and 5), and those of neurodegeneration such as SMI32 (Figure 6) were increased after LPS injection, and the levels were reduced in the conditions where CD38 was deleted or inhibited, and $NAD^+$ synthesis was supported by precursor supplementation. Since proinflammatory genes were elevated at earlier stages than glial markers after LPS administration, it is likely that the suppressive effects on glial activation are secondary to the anti-inflammatory effect of CD38 deletion or inhibition, and support of $NAD^+$ synthesis. However, we cannot rule out the possibility that CD38 directly regulates glial activation, since CD38 enhances GFAP expression during the postnatal development stages in vivo (Hattori et al., 2017).

In contrast to the potential mechanisms by which CD38 and calcium release promote inflammatory gene expression, CD38 inhibition and NR supplementation both converge on elevated $NAD^+$- mediated

suppression of inflammatory responses. We recently showed that coronavirus infection induces transcriptional induction of a set of PARP-related genes that depleted cellular $NAD^+$ and that supplementation with $NAD^+$ precursors or pharmacological activation of $NAD^+$ synthesis can boost the activity of the highly transcribed PARP genes while providing partial protection against viral replication (Heer et al., 2020). Here, we show that many of the same PARP genes are up-regulated after LPS stimulation in vitro and in vivo (Figure S1). We therefore suggest that depressed activities of NAD-dependent enzymes (other than CD38) mediate inflammatory gene transcription. Three potential mediators are SIRT2, which reportedly prevents microglial activation by promoting NF-κB deacetylation (Pais et al., 2013), SIRT1, which potentially depresses NF-κB activity via deacetylation of p65/RelaA (Caon et al., 2020) and PARP10, which inhibit activation of NF-κB and downstream target genes in response to IL-1β and TNF-α in a manner that depends on its catalytic activity and poly-ubiquitin binding activities (Verheugd et al., 2013). As glia-derived cytokines such as IFN-γ and TNF-α synergistically promote neuronal degeneration with other toxic factors (Suzumura et al., 2006), the reduced levels of neuronal damage by NR or apigenin administration are likely attributed to decreased induction of pro-inflammatory molecules. Consistent with this proposed mechanism, three weeks of oral high-dose NR has been shown to depress the circulation of inflammatory cytokines in a small placebo-controlled trial of older men (Elhassan et al., 2019). $NAD^+$ may also protect neurons directly because $NAD^+$ degradation has been directly linked to axonal degeneration. Sterile alpha and the TIR motif containing 1 (SARM1) initiates a local destruction program of axons through a process that involves the catastrophic depletion of axonal $NAD^+$ (Essuman et al., 2017).

These results are not without caveats. For example, apigenin showed stronger effects than other compounds such as NR and 78c to suppress *Il6* and *Nos2* in cultured microglia and *Il6* in cultured astrocytes (Figure 7). Moreover apigenin decreased cytokine expression even in LPS-injected CD38 KO mice (Figure 4h–j), suggesting that it has targets beyond CD38, which could include MAPK, Akt, JNK (Ginwala et al., 2019) or the GSK3b/Nrf2 signaling pathway (Chen et al., 2019).

## 4.2 | Future prospects

Neuroinflammation is a contributing factor in various neurodegenerative diseases including Alzheimer's disease and Parkinson's disease (Ginwala et al., 2019; Glass et al., 2010). Importantly, the vulnerability of hippocampal neurons that leads to cognitive impairment is strongly associated with neuroinflammation (Semmler et al., 2013; Tan et al., 2014). In fact, apigenin and NR have been reported to have beneficial effects on neurodegenerative disease models (Hou et al., 2018; Zhao et al., 2013). Apigenin has been reported to cross the blood–brain barrier (BBB) and increase $NAD^+$ concentration in the brain (Balez et al., 2016). NR can also increase $NAD^+$ levels in the brains of Alzheimer's disease model mice when orally administered (Gong et al., 2013). In ongoing work, we aim to clarify the neuroprotective mechanisms in disease models such as multiple sclerosis and Parkinson's disease models in order to better identify biomarkers that will enable successful clinical translation.

We identified novel effects of NR and apigenin on LPS-induced neuroinflammation. Testing these compounds in neurodegenerative diseases, aging, and neurodevelopmental disease models may be important for the development of new therapies for these diseases.

## ACKNOWLEDGEMENT

The authors thank Mr. Takashi Tamatani for providing technical assistance and ChromaDex for Niagen. This work was supported by Grant-in Aid for Scientific Research (18KK0435, 18K06501 for TH, 18KK0255, 18K06500 for OH, and 18K06463 for MT) from the Ministry of Education, Science, Technology, Sports and Culture of Japan, by Alfred E. Mann Family Foundation (for CB), by National Cancer Institute (F99CA245722 for CH) and by Kanazawa University SAKIGAKE Project 2018 and the CHOZEN project. A preprint was posted on ResearchSquare on 28 Dec 2020 (https://www.researchsquare.com/article/rs-135107/v1).

All experiments were conducted in compliance with the ARRIVE guidelines.

## CONFLICT OF INTEREST

The authors declare that they have no competing interests.

## AUTHORS' CONTRIBUTIONS

JR, TH, CB, and OH conceived and designed the experiments. JR, HI, MT, CH, and DM performed the experiments and analyzed the data. JR, TH, CB, and OH wrote the paper. JR, TH, CB, YY, HO, HH, and OH discussed the data. All authors have read and approved the paper.

## DATA AVAILABILITY STATEMENT

The data that support the findings of this study are available in Gene Expression Omnibus (GEO) at https://www.ncbi.nlm.nih.gov/geo/, reference number GSE49329, GSE102482, and GSE122815. This article has been published as a Preprint on https://www.researchsquare.com/article/rs-135107/v1

## ORCID

*Tsuyoshi Hattori* https://orcid.org/0000-0002-8168-8710
*Osamu Hori* https://orcid.org/0000-0002-2210-0446

## REFERENCES

Akiyama, H., Barger, S., Barnum, S., Bradt, B., Bauer, J., Cole, G. M., Cooper, N. R., Eikelenboom, P., Emmerling, M., Fiebich, B. L., & Finch, C. E. (2000). Inflammation and Alzheimer's disease. *Neurobiology of Aging*, *21*, 383–421. https://doi.org/10.1016/S0197-4580(00)00124-X

Balez, R., Steiner, N., Engel, M., Muñoz, S. S., Lum, J. S., Wu, Y., … Ooi, L. (2016). Neuroprotective effects of apigenin against inflammation, neuronal excitability and apoptosis in an induced pluripotent stem cell model of Alzheimer's disease. *Scientific Reports*, *6*, 31450. https://doi.org/10.1038/srep31450

Bieganowski, P. & Brenner, C. (2004). Discoveries of nicotinamide riboside as a nutrient and conserved NRK genes establish a Preiss-Handler independent route to NAD+ in fungi and humans. *Cell*, *117*, 495–502. https://doi.org/10.1016/S0092-8674(04)00416-7

Blacher, E., Dadali, T., Bespalko, A., Haupenthal, V. J., Grimm, M. O., Hartmann, T., … Levy, A. (2015). Alzheimer's disease pathology is attenuated in a CD38-deficient mouse model. *Annals of Neurology*, *78*, 88–103. https://doi.org/10.1002/ana.24425

Bogan, K. L. & Brenner, C. (2008). Nicotinic acid, nicotinamide, and nicotinamide riboside: A molecular evaluation of $NAD^+$ precursor vitamins in human nutrition. *Annual Review of Nutrition*, *28*, 115–130.

Caon, I., Bartolini, B., Moretto, P., Parnigoni, A., Caravà, E., Vitale, D. L., Alaniz, L., Viola, M., Karousou, E., De Luca, G., & Hascall, V. C. (2020). Sirtuin 1 reduces hyaluronan synthase 2 expression by inhibiting nuclear translocation of NF-kB and expression of the long-non coding RNA HAS2-AS1. *The Journal of Biological Chemistry*, *295*(11), 3485–3496.

Chen, P., Huo, X., Liu, W., Li, K., Sun, Z., & Tian, J. (2019). Apigenin exhibits anti-inflammatory effects in LPS-stimulated BV2 microglia through activating GSK3beta/Nrf2 signaling pathway. *Immunopharmacology and Immunotoxicology*, *42*(1), 9–16.

Chini, C. C. S., Peclat, T. R., Warner, G. M., Kashyap, S., Espindola-Netto, J. M., de Oliveira, G. C., & Chini, E. N. (2020). CD38 ecto-enzyme in immune cells is induced during aging and regulates NAD(+) and NMN levels. *Nature Metabolism*, *2*, 1284–1304. https://doi.org/10.1038/s42255-020-00298-z

Davis, S. & Meltzer, P. S. (2007). GEOquery: A bridge between the gene expression omnibus (GEO) and BioConductor. *Bioinformatics*, *23*, 1846–1847. https://doi.org/10.1093/bioinformatics/btm254

Deng, X., Li, M., Ai, W., He, L., Lu, D., Patrylo, P. R., … Yan, X.-X. (2014). Lipolysaccharide-induced neuroinflammation is associated with Alzheimer-like amyloidogenic axonal pathology and dendritic degeneration in rats. *Advances in Alzheimer's Disease*, *3*, 78–93. https://doi.org/10.4236/aad.2014.32009

Diguet, N., Trammell, S. A. J., Tannous, C., Deloux, R., Piquereau, J., Mougenot, N., … Mericskay, M. (2018). Nicotinamide riboside preserves cardiac function in a mouse model of dilated cardiomyopathy. *Circulation*, *137*, 2256–2273. https://doi.org/10.1161/CIRCULATIONAHA.116.026099

Elhassan, Y. S., Kluckova, K., Fletcher, R. S., Schmidt, M. S., Garten, A., Doig, C. L., & Lavery, G. G. (2019). Nicotinamide riboside augments the aged human skeletal muscle NAD(+) Metabolome and induces transcriptomic and anti-inflammatory signatures. *Cell Reports*, *28*(7), 1717–1728.e6. https://doi.org/10.1016/j.celrep.2019.07.043

Escande, C., Nin, V., Price, N. L., Capellini, V., Gomes, A. P., Barbosa, M. T., … Chini, E. N. (2013). Flavonoid apigenin is an inhibitor of the $NAD^+$ase CD38: Implications for cellular $NAD^+$ metabolism, protein acetylation, and treatment of metabolic syndrome. *Diabetes*, *62*, 1084–1093. https://doi.org/10.2337/db12-1139

Essuman, K., Summers, D. W., Sasaki, Y., Mao, X., DiAntonio, A., & Milbrandt, J. (2017). The SARM1 Toll/Interleukin-1 receptor domain possesses intrinsic NAD(+) cleavage activity that promotes pathological axonal degeneration. *Neuron*, *93*(1334–1343), e1335. https://doi.org/10.1016/j.neuron.2017.02.022

Frischer, J. M., Bramow, S., Dal-Bianco, A., Lucchinetti, C. F., Rauschka, H., Schmidbauer, M., … Lassmann, H. (2009). The relation between inflammation and neurodegeneration in multiple sclerosis brains. *Brain*, *132*, 1175–1189. https://doi.org/10.1093/brain/awp070

Gerasimenko, M., Cherepanov, S. M., Furuhara, K., Lopatina, O., Salmina, A. B., Shabalova, A. A., … Higashida, H. (2020). Nicotinamide riboside supplementation corrects deficits in oxytocin, sociability and anxiety of CD157 mutants in a mouse model of autism spectrum disorder. *Scientific Reports*, *10*, 10035. https://doi.org/10.1038/s41598-019-57236-7

Ginwala, R., Bhavsar, R., Chigbu, D. I., Jain, P., & Khan, Z. K. (2019). Potential role of flavonoids in treating chronic inflammatory diseases with a special focus on the anti-inflammatory activity of apigenin. *Antioxidants*, *8*. https://doi.org/10.3390/antiox8020035

Glass, C. K., Saijo, K., Winner, B., Marchetto, M. C., & Gage, F. H. (2010). Mechanisms underlying inflammation in neurodegeneration. *Cell*, *140*, 918–934. https://doi.org/10.1016/j.cell.2010.02.016

Gong, B., Pan, Y., Vempati, P., Zhao, W., Knable, L., Ho, L., Wang, J., Sastre, M., Ono, K., Sauve, A. A., & Pasinetti, G. M. (2013). Nicotinamide riboside restores cognition through an upregulation of proliferator-activated receptor-gamma coactivator 1alpha regulated beta-secretase 1 degradation and mitochondrial gene expression in Alzheimer's mouse models. *Neurobiology of Aging*, *34*, 1581–1588.

Guse, A. H. (2005). Second messenger function and the structure-activity relationship of cyclic adenosine diphosphoribose (cADPR). *FEBS Journal*, *272*, 4590–4597. https://doi.org/10.1111/j.1742-4658.2005.04863.x

Hattori, T., Kaji, M., Ishii, H., Jureepon, R., Takarada-Iemata, M., Minh Ta, H., … Hori, O. (2017). CD38 positively regulates postnatal development of astrocytes cell-autonomously and oligodendrocytes non-cell-autonomously. *Glia*, *65*, 974–989. https://doi.org/10.1002/glia.23139

Hattori, T., Shimizu, S., Koyama, Y., Yamada, K., Kuwahara, R., Kumamoto, N., … Tohyama, M. (2010). DISC1 regulates cell-cell adhesion, cell-matrix adhesion and neurite outgrowth. *Molecular Psychiatry*, *15*(778), 798–809. https://doi.org/10.1038/mp.2010.60

Heer, C. D., Sanderson, D. J., Voth, L. S., Alhammad, Y. M., Schmidt, M. S., Trammell, S. A., Perlman, S., Cohen, M. S., Fehr, A. R., & Brenner, C. (2020). Coronavirus infection and PARP expression dysregulate the NAD Metabolome: An actionable component of innate immunity. *The Journal of Biological Chemistry*, *295*(52), 17986–17996.

Herrmann, M. M., Barth, S., Greve, B., Schumann, K. M., Bartels, A., & Weissert, R. (2016). Identification of gene expression patterns crucially involved in experimental autoimmune encephalomyelitis and multiple sclerosis. *Disease Models & Mechanisms*, *9*, 1211–1220. https://doi.org/10.1242/dmm.025536

Higashida, H., Yokoyama, S., Kikuchi, M., & Munesue, T. (2012). CD38 and its role in oxytocin secretion and social behavior. *Hormones and Behavior*, *61*, 351–358. https://doi.org/10.1016/j.yhbeh.2011.12.011

Hogan, K. A., Chini, C. C. S., & Chini, E. N. (2019). The multi-faceted ecto-enzyme CD38: Roles in immunomodulation, cancer, aging, and metabolic diseases. *Frontiers in Immunology*, *10*, 1187. https://doi.org/10.3389/fimmu.2019.01187

Hou, Y., Lautrup, S., Cordonnier, S., Wang, Y., Croteau, D. L., Zavala, E., Zhang, Y., Moritoh, K., O'Connell, J. F., Baptiste, B. A., & Stevnsner, T. V. (2018). NAD(+) supplementation normalizes key Alzheimer's features and DNA damage responses in a new AD mouse model with introduced DNA repair deficiency. *Proceedings of the National Academy of Sciences of the United States of America*, *115*, E1876–E1885.

Jin, D., Liu, H.-X., Hirai, H., Torashima, T., Nagai, T., Lopatina, O., & Higashida, H. (2007). CD38 is critical for social behaviour by regulating oxytocin secretion. *Nature*, *446*, 41–45. https://doi.org/10.1038/nature05526

Jo, M., Kim, J. H., Song, G. J., Seo, M., Hwang, E. M., & Suk, K. (2017). Astrocytic orosomucoid-2 modulates microglial activation and neuroinflammation. *Journal of Neuroscience*, *37*, 2878–2894. https://doi.org/10.1523/JNEUROSCI.2534-16.2017

Kato, I., Yamamoto, Y., Fujimura, M., Noguchi, N., Takasawa, S., & Okamoto, H. (1999). CD38 disruption impairs glucose-induced increases in cyclic ADP-ribose, [Ca2+]i, and insulin secretion. *Journal of Biological Chemistry*, *274*, 1869–1872.

Kim, S., Kim, T. H., Lee, H.-R., Jang, E.-H., Ryu, H.-H., Kang, M., … Kaang, B.-K. (2016). Impaired learning and memory in CD38 null mutant mice. *Molecular Brain*, *9*, 16. https://doi.org/10.1186/s13041-016-0195-5

Lee, H. C. (2004). Multiplicity of $Ca^{2+}$ messengers and $Ca^{2+}$ stores: A perspective from cyclic ADP-ribose and NAADP. *Current Molecular Medicine*, *4*, 227–237.

Lian, H., Litvinchuk, A., Chiang, A. C., Aithmitti, N., Jankowsky, J. L., & Zheng, H. (2016). Astrocyte-microglia cross talk through complement activation modulates amyloid pathology in mouse models of Alzheimer's disease. *Journal of Neuroscience*, *36*, 577–589. https://doi.org/10.1523/JNEUROSCI.2117-15.2016

Liu, W., Tang, Y., & Feng, J. (2011). Cross talk between activation of microglia and astrocytes in pathological conditions in the central nervous system. *Life Sciences*, *89*, 141–146. https://doi.org/10.1016/j.lfs.2011.05.011

Lucas, S. M., Rothwell, N. J., & Gibson, R. M. (2006). The role of inflammation in CNS injury and disease. *British Journal of Pharmacology*, *147*(Suppl 1), S232–240. https://doi.org/10.1038/sj.bjp.0706400

Malavasi, F., Deaglio, S., Funaro, A., Ferrero, E., Horenstein, A. L., Ortolan, E., … Aydin, S. (2008). Evolution and function of the ADP ribosyl cyclase/CD38 gene family in physiology and pathology. *Physiological Reviews*, *88*, 841–886. https://doi.org/10.1152/physrev.00035.2007

Nam, T. S., Park, D. R., Rah, S. Y., Woo, T. G., Chung, H. T., Brenner, C., & Kim, U. H. (2020). Interleukin-8 drives CD38 to form NAADP from NADP(+) and NAAD in the endolysosomes to mobilize Ca(2+) and effect cell migration. *FASEB Journal: Official Publication of the Federation of American Societies for Experimental Biology*, *34*(9), 12565–12576.

Nijveldt, R. J., van Nood, E., van Hoorn, D. E., Boelens, P. G., van Norren, K., & van Leeuwen, P. A. (2001). Flavonoids: A review of probable mechanisms of action and potential applications. *American Journal of Clinical Nutrition*, *74*, 418–425. https://doi.org/10.1093/ajcn/74.4.418

Norden, D. M., Trojanowski, P. J., Villanueva, E., Navarro, E., & Godbout, J. P. (2016). Sequential activation of microglia and astrocyte cytokine expression precedes increased Iba-1 or GFAP immunoreactivity following systemic immune challenge. *Glia*, *64*, 300–316. https://doi.org/10.1002/glia.22930

Okamoto, H., Takasawa, S., & Yamamoto, Y. (2017). From insulin synthesis to secretion: Alternative splicing of type 2 ryanodine receptor gene is essential for insulin secretion in pancreatic beta cells. *The International Journal of Biochemistry & Cell Biology*, *91*, 176–183.

Pais, T. F., Szego, E. M., Marques, O., Miller-Fleming, L., Antas, P., Guerreiro, P., … Outeiro, T. F. (2013). The NAD-dependent deacetylase sirtuin 2 is a suppressor of microglial activation and brain inflammation. *The EMBO Journal*, *32*, 2603–2616. https://doi.org/10.1038/emboj.2013.200

Pintado, C., Gavilan, M. P., Gavilan, E., Garcia-Cuervo, L., Gutierrez, A., Vitorica, J., … Ruano, D. (2012). Lipopolysaccharide-induced neuroinflammation leads to the accumulation of ubiquitinated proteins and increases susceptibility to neurodegeneration induced by proteasome inhibition in rat hippocampus. *Journal of Neuroinflammation*, *9*, 87. https://doi.org/10.1186/1742-2094-9-87

Qin, L., Wu, X., Block, M. L., Liu, Y., Breese, G. R., Hong, J. S., … Crews, F. T. (2007). Systemic LPS causes chronic neuroinflammation and progressive neurodegeneration. *Glia*, *55*, 453–462. https://doi.org/10.1002/glia.20467

Ritchie, M. E., Phipson, B., Wu, D., Hu, Y., Law, C. W., Shi, W., & Smyth, G. K. (2015). limma powers differential expression analyses for RNA-sequencing and microarray studies. *Nucleic Acids Research*, *43*, e47. https://doi.org/10.1093/nar/gkv007

Roboon, J., Hattori, T., Ishii, H., Takarada-Iemata, M., Le, T. M., Shiraishi, Y., … Hori, O. (2019). Deletion of CD38 suppresses glial activation and neuroinflammation in a mouse model of demyelination. *Frontiers in Cellular Neuroscience*, *13*, 258. https://doi.org/10.3389/fncel.2019.00258

Semmler, A., Widmann, C. N., Okulla, T., Urbach, H., Kaiser, M., Widman, G., … Heneka, M. T. (2013). Persistent cognitive impairment, hippocampal atrophy and EEG changes in sepsis survivors. *Journal of Neurology, Neurosurgery, and Psychiatry*, *84*, 62–69. https://doi.org/10.1136/jnnp-2012-302883

Shukla, S. & Gupta, S. (2010). Apigenin: A promising molecule for cancer prevention. *Pharmaceutical Research*, *27*, 962–978. https://doi.org/10.1007/s11095-010-0089-7

Suzumura, A., Takeuchi, H., Zhang, G., Kuno, R., & Mizuno, T. (2006). Roles of glia-derived cytokines on neuronal degeneration and regeneration. *Annals of the New York Academy of Sciences*, *1088*, 219–229. https://doi.org/10.1196/annals.1366.012

Takasawa, S., Nata, K., Yonekura, H., & Okamoto, H. (1993a). Cyclic ADP-ribose in insulin secretion from pancreatic beta cells. *Science*, *259*, 370–373. https://doi.org/10.1126/science.8420005

Takasawa, S., Nata, K., Yonekura, H., & Okamoto, H. (1993b). Response. *Science*, *262*, 585. https://doi.org/10.1126/science.262.5133.585

Takasawa, S., Tohgo, A., Noguchi, N., Koguma, T., Nata, K., Sugimoto, T., … Okamoto, H. (1993c). Synthesis and hydrolysis of cyclic ADP-ribose by human leukocyte antigen CD38 and inhibition of the hydrolysis by ATP. *The Journal of Biological Chemistry*, *268*, 26052–26054. https://doi.org/10.1016/S0021-9258(19)74275-6

Tan, H., Cao, J., Zhang, J., & Zuo, Z. (2014). Critical role of inflammatory cytokines in impairing biochemical processes for learning and memory after surgery in rats. *Journal of Neuroinflammation*, *11*, 93. https://doi.org/10.1186/1742-2094-11-93

Tarragó, M. G., Chini, C. C. S., Kanamori, K. S., Warner, G. M., Caride, A., de Oliveira, G. C., … Chini, E. N. (2018). A potent and specific CD38 inhibitor ameliorates age-related metabolic dysfunction by reversing tissue NAD(+) decline. *Cell Metabolism*, *27*(5), 1081–1095.e10. https://doi.org/10.1016/j.cmet.2018.03.016

Trammell, S. A. J., Schmidt, M. S., Weidemann, B. J., Redpath, P., Jaksch, F., Dellinger, R. W., … Brenner, C. (2016). Nicotinamide riboside is uniquely and orally bioavailable in mice and humans. *Nature Communications*, *7*, 12948. https://doi.org/10.1038/ncomms12948

Vaur, P., Brugg, B., Mericskay, M., Li, Z., Schmidt, M. S., Vivien, D., Orset, C., Jacotot, E., Brenner, C., & Duplus, E. (2017). Nicotinamide riboside, a form of vitamin B3, protects against excitotoxicity-induced axonal degeneration. *The FASEB Journal*, *31*, 5440–5452.

Venigalla, M., Gyengesi, E., & Munch, G. (2015). Curcumin and Apigenin – Novel and promising therapeutics against chronic neuroinflammation in Alzheimer's disease. *Neural Regeneration Research*, *10*, 1181–1185. https://doi.org/10.4103/1673-5374.162686

Verheugd, P., Forst, A. H., Milke, L., Herzog, N., Feijs, K. L., Kremmer, E., … Luscher, B. (2013). Regulation of NF-kappaB signalling by the mono-ADP-ribosyltransferase ARTD10. *Nature Communications*, *4*, 1683.

Wang, Y., Ni, J., Zhai, L., Gao, C., Xie, L., Zhao, L., & Yin, X. (2019). Inhibition of activated astrocyte ameliorates lipopolysaccharide- induced depressive-like behaviors. *Journal of Affective Disorders*, *242*, 52–59. https://doi.org/10.1016/j.jad.2018.08.015

Zhao, J., Bi, W., Xiao, S., Lan, X., Cheng, X., Zhang, J., … Zhu, L. (2019). Neuroinflammation induced by lipopolysaccharide causes cognitive impairment in mice. *Scientific Reports*, *9*, 5790. https://doi.org/10.1038/s41598-019-42286-8

Zhao, L., Wang, J. L., Liu, R., Li, X. X., Li, J. F., & Zhang, L. (2013). Neuroprotective, anti-amyloidogenic and neurotrophic effects of apigenin in an Alzheimer's disease mouse model. *Molecules*, *18*, 9949–9965. https://doi.org/10.3390/molecules18089949

Zhao, Y. J., Lam, C. M., & Lee, H. C. (2012). The membrane-bound enzyme CD38 exists in two opposing orientations. *Science Signaling*, *5*, ra67. https://doi.org/10.1126/scisignal.2002700

## SUPPORTING INFORMATION

Additional supporting information may be found online in the Supporting Information section.

**How to cite this article:** Roboon J, Hattori T, Ishii H, et al. Inhibition of CD38 and supplementation of nicotinamide riboside ameliorate lipopolysaccharide-induced microglial and astrocytic neuroinflammation by increasing $NAD^+$. *J Neurochem*. 2021;158:311–327. https://doi.org/10.1111/jnc.15367